

ALPTHERM – A PC-BASED MODEL FOR ATMOSPHERIC CONVECTION OVER COMPLEX TOPOGRAPHY

by O.Liechti, Analysen& Konzepte, Switzerland
and B. Neininger, MetAir AG, Switzerland

Presented at the XXIII OSTIV Congress, Borlänge, Sweden (1993)

Introduction

Forecasting soaring flight conditions in mountainous areas is more complex than over flat terrain due to the area-height distribution (AHD) of topography - imagine a mountain valley sliced into horizontal layers of constant thickness and plot the ratio of topographic to atmospheric surface area versus height (Figure 1). First the atmospheric volume fraction of the horizontal layers increases from the bottom of the valley (0%) to the top (100%) and remains constant above the topography. Secondly, the AHD introduces a vertical distribution of the atmospheric heating (and cooling) since solar radiation hits the ground at different altitudes. In a valley the atmospheric volume fraction and the surface area are functions of height. Over a plain the atmospheric volume of the layers is always 100%. This volume effect (Steinacker 1984, Neininger 1982, 1983) is the reason why the apparent input of sensible heat is larger over mountain valleys than over flat terrain. Or, to put it differently: in a

valley the atmospheric heat capacity per layer increases with height. If the layer volume varies with altitude the emagram loses its proportionality of area to energy in those layers for which the volume is not 100%. The

maximum day temperature in a mountain valley can still be estimated by the Gold method if the volume effect is considered. As a rule of thumb it was found for the Alps that the maximum day temperature at the bottom of the valley decreases by about 5°C if the valley floor rises by 1000 m (Truog, 1979).

In order to assess the dynamics and the precise temporal evolution of convection the use of computers becomes advisable, in particular if topography should be considered. This was the starting point for the development of <<ALPTHERM>>. Apart from dynamics the vertical exchange and mixing of air parcels can be obtained quantitatively from a numerical convection model. Such information is crucial in air quality issues. Whiteman's idealized analytical model (1982) of the

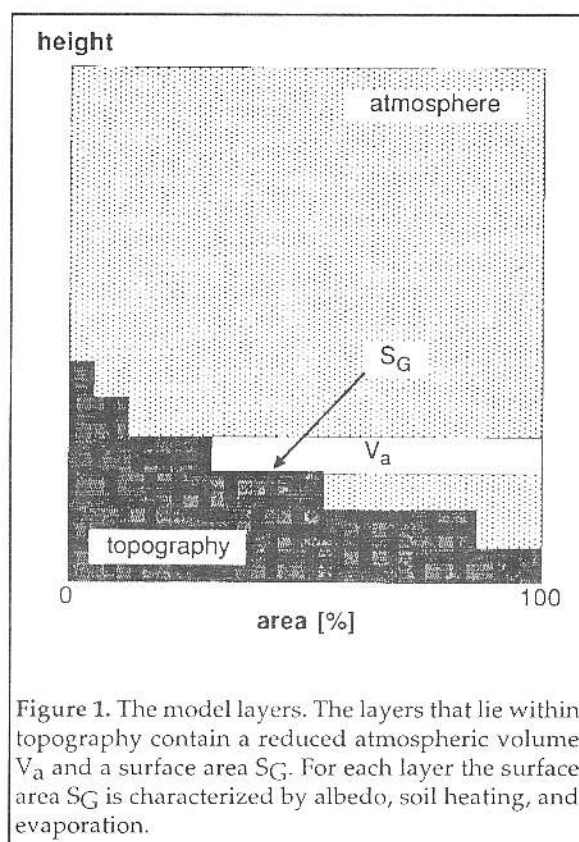


Figure 1. The model layers. The layers that lie within topography contain a reduced atmospheric volume V_a and a surface area S_G . For each layer the surface area S_G is characterized by albedo, soil heating, and evaporation.

vertical mixing in a valley atmosphere needs only a pocket calculator. It inspired us to develop a dynamic convection model for complex topography that uses a PC.

Model physics: Topography, Radiation, and Dynamics

On a topographic map a region of a few 100 km² is chosen. In mountainous terrain the region could typically be a valley section of length about 10 km delimited by the ridges on either side. Over hills and plains it is sufficient to choose a region with a representative area-height distribution. The atmosphere over the selected region is sliced into horizontal layers of constant thickness (Figure 1). Each layer has a surface area S_G that must be deduced from the map or from digital topography data. Given the surface area of all layers the atmospheric volume V_a of the layers can be computed. Above the topography no surfaces are present any more and the layer volume remains constant. In terms of geometry <<ALPHERM>> is a two-dimensional model. Vertically the resolution is fixed (ie. 100 m), horizontally the resolution is variable according to the number of layers with topographic volume parts (1 layer for a plain, typically 20 layers in the Alps). Each layer surface is assigned surface characteristics: albedo, ground heating and evaporation. These parameters will vary slightly with the seasons.

The sun's elevation ε is a function of latitude φ, of the inclination η of the earth's axis to the ecliptic, of the position β of the earth in its orbit around the sun, and the position α of the earth in its rotation about its poles:

$$\sin(\epsilon) = \sin(\phi) \cdot \sin(\eta) \cdot \cos(\beta) - \cos(\phi) \cdot \cos(\eta) \cdot \cos(\beta) \cdot \sin(\alpha) + \cos(\phi) \cdot \sin(\beta) \cdot \cos(\alpha) \quad (1)$$

(β) represents the annual and α the daily variation of the solar elevation at a given latitude φ. The longitude λ of the region and the time zone enter into the offset of α. The intensity of the solar radiation is reduced by atmospheric reflectivity and attenuation. These effects are particularly important for correct intensities at low elevations for which the optical path length increases drastically. In the model the atmospheric transmission T at the altitude z is obtained from the formulas

$$T(z) = \exp[-\Gamma \cdot \sin(\epsilon_{\max}) / \sin(\epsilon)] \quad (2a)$$

$$\Gamma = \Gamma_{\max} \cdot \exp[-z / z_{\Gamma}] \quad (2b)$$

ε_{max} is the sun's elevation at noon. Γ_{max} = 0.323 = ln(0.74) and z_Γ = 2333 m are constants obtained by fitting data found in Häckel. The intensity S of incoming radiation depends on the sun's elevation and on the altitude:

$$S = S_0 \cdot \sin(\epsilon) \cdot T(z) \quad (3)$$

(S₀ = 1200 W/m²). S is illustrated for mid-latitudes in Figure 2 for various altitudes and seasons. The absorbed radiation Q_k at altitude z is computed as

$$Q_k = S \cdot (1 - A) \quad (4)$$

for a clear sky with A as albedo of the layer. A typical value for A is 15%. The outgoing radiation Q_f is calculated from the black body radiation and the atmosphere back radiation

$$Q_f = \sigma \cdot (T_S^4 - \mu \cdot T_A^4) \quad (5)$$

σ = 5.67 • 10⁻⁸ W/m²K⁴, T_S = soil temperature, T_A = air temperature at 2 m above ground. μ reflects the influence of humidity on the atmosphere back radiation through the vapor pressure e given in hPa:

$$\mu = 0.594 + 0.0416 \cdot e^{0.5} \quad (6)$$

(from Baur & Philips (1934) in Häckel, p. 154). The radiation budget P is obtained as

$$P = Q_k - Q_f \quad (7)$$

The difference between the soil temperature T_S used in (5) and the air temperature T_A is chosen to be proportional to the radiation budget P

$$T_S - T_A = \delta \cdot P \quad (8)$$

with δ = 0.005 K • m²/W. At daytime a positive radiation budget P is divided into fluxes of ground heat (1 - G) • P, latent heat P_{lat}, and sensible heat P_{sens}

$$P_{\text{lat}} = \text{Evap} \cdot (1 - G) \cdot P \quad (9)$$

$$P_{\text{sens}} = (1 - \text{Evap}) \cdot (1 - G) \cdot P \quad (10)$$

Typical values found for the Swiss plateau (latitude 47°, cultivated land, height 400 - 700 mASL) are Evap = 60% and G = 15%.

At this point some assumptions are made in order to assess the dynamics of vertical motion. The model is based on a constant time step of Δt = 120 sec. Given the flux of sensible heat P_{sens}, the time step Δt, and the surface area S_G of the layer the sensible heat H_{sens} fed into the layer's surface air is

$$H_{\text{sens}} = P_{\text{sens}} \cdot \Delta t \cdot S_G \quad (11)$$

For the dynamics it is crucial to know the temperature difference ΔT between the heated air parcels and the free atmosphere. Reasonable lift rates are obtained with the following method that distinguishes between two regimes:

$$\Delta T = \Delta T_0 \cdot P_{\text{sens}} / P_0 \text{ if } P_{\text{sens}} < P_0 \quad (12a)$$

$$\Delta T = \Delta T_0 \text{ if } P_{\text{sens}} \geq P_0 \quad (12b)$$

For small fluxes of sensible heat the temperature difference is proportional to the flux. Above the threshold value $P_0 = 75 \text{ W/m}^2$ the temperature difference is limited to $\Delta T_0 = 0.5 \text{ K}$. It should be pointed out, that this is the average temperature difference of the heated air across the full depth Δz of a layer, ie. 100 m. Superadiabatic gradients close to the ground may show much larger temperature differences between the air temperature measured at 2 m and the temperature of the mixed free atmosphere extrapolated down along the dry adiabat to the same height. Given the sensible heat (11) and the temperature difference (12) it is straightforward to calculate the mass of the heated air parcel:

$$m_p = H_{\text{sens}} / C_p / dT \quad (13)$$

($C_p = 1005 \text{ J / kg / K}$). The amount of evaporated water is obtained by

$$m_{\text{water}} = H_{\text{lat}} / L \quad (14)$$

with $L = 2500 \text{ kJ / kg}$, $H_{\text{lat}} = P_{\text{lat}} \cdot \Delta t - S_G$. So radiation produces air parcels of given mass in each layer with an increased temperature and humidity with respect to the free atmosphere.

Due to buoyancy these air parcels will move vertically. Their gain of energy per unit mass dE / m_p on a transition from layer n to the next higher layer $n + 1$ is

$$dE / m_p = g \cdot \Delta z \cdot ((\rho_f^{[n+1]} / \rho_p^{[n+1]} + \rho_f^{[n]} / \rho_p^{[n]}) / 2 - 1) \quad (15)$$

where ρ_f and ρ_p are the densities of the free atmosphere and the air parcel, respectively. The density of the air parcel at the new layer must be computed under consideration of condensation (cloud formation). As long as the sum of all transition energies

$$E/m = \sum (dE / m_p)_{n \rightarrow n+1} \quad (16)$$

is positive the parcel is allowed to rise. The vertical velocity v of the air parcel at a given layer is simply

$$v = (2 \cdot E / m)^{0.5} \quad (17)$$

It is important to allow for entrainment and detrainment during the transitions in order to obtain reasonable motion. The entrainment/detrainment factors per transition are proportional to the velocity:

$$E_n = E_{n0} \cdot |v| \quad (18a)$$

$$D_e = D_{e0} \cdot |v| \quad (18b)$$

with $E_{n0} = D_{e0} = 0.02 \text{ (m/s)}^{-1}$ during acceleration and $E_{n0} = D_{e0} = 0.08 \text{ (m/s)}^{-1}$ during slowing down.

From gliding it is known that horizontal winds reduce the lift rates. A rough parametrization of this reduction is implemented in <<ALPTHERM>>. Horizontal winds in the convection layer are likely to affect the entrainment/detrainment factors E_n and D_e . However, a simpler approach is used in <<ALPTHERM>>. The gain in kinetic energy (15) is multiplied by a kinetic conversion factor

$$f_{\text{kin}} = 1 - r \cdot u^2 \quad (19)$$

that depends on the average horizontal wind ($r = 1.65e - 4 \text{ (km/h)}^{-2}$). For $u = 60 \text{ km/h}$, eg., the kinetic conversion factor is reduced to 0.4 and vertical velocities v are reduced to 63% of the values obtained for calm conditions. The form of (19) implies that light winds do practically not affect lift rates. The value used for r is a guess. No attempts to verify this value of r have been made so far.

Each air parcel will eventually find its equilibrium layer into which it is mixed. Its mass and water content, its latent and sensible heat are added to the equilibrium layer. The final result is an upward transport of all these quantities. At the ground the mass deficit must be compensated by subsidence of the free atmosphere. At this point it is also possible to treat synoptic changes of the temperature and humidity profile due to advection or large scale subsidence. This cycle of heating, turbulent vertical motion and subsidence is repeated for the full day.

Representative profiles

The model must be started with an early morning temperature and humidity profile that is representative for the region under consideration. In Switzerland there are two sources of data available: radiosounding data taken at 02 a.m. (local time) and data from a national network of ground stations (readings at sunrise, stations at altitudes between 200 and 3600 mASL). The following superposition of both data proved to give good results: within topography, the ground stations within the region are given fixed weight and the weight of the radiosounding data decreases from the top down to the bottom of the topography; above the topography, the radiosounding data are given fixed weight and the station data are given individual weights according to their distance to the region (Table 1, Figure 2).

Model Results

The lift rates for sailplanes flying in thermals at a particular altitude are obtained from the averaged vertical velocities of all air parcels crossing this altitude minus the sink rate (ie. 1 m/s) of the planes while spiraling. In addition to time height cross-sections of lift rates (Figure 3) the model also provides quantitative results on convective clouds: the base and top height of cumulus clouds and the cloud cover in each layer. The

RADIOSONDE 02H PAYERNE

HEIGHT | T | TD

0500	+09	+06
0800	+13	07
1500	+09	+02
2100	+06	-18
3000	+00	-12
4200	-09	-15
4800	-11	-22
5000	-12	-22

STATIONS 08H Voralpen

HEIGHT | T | Td | W | STATION

400	08	6	1	Buchs-Suhr
800	11	6	1	Laegern
1100	12	6	1	Hoernli
1400	11	4	1	Napf
1600	9.5	1	1	Chasseral
2000	7	-1	5	Molésón
2100	6	-1	5	Pilatus
2300	4.5	1	5	Gütsch
3600	-5	-8	5	Jungfrauoch
4200	-9	-15	1	Sondenpunkt

Table 1. Input data for <<ALPTHERM>>: radiosonde and ground stations.

figure shows the evolution of the vertical profiles of temperature and humidity during the day and to observe the predicted time series of ground temperature and dew point. Characteristic points like the breaking of inversions can be identified with temperature. The dew

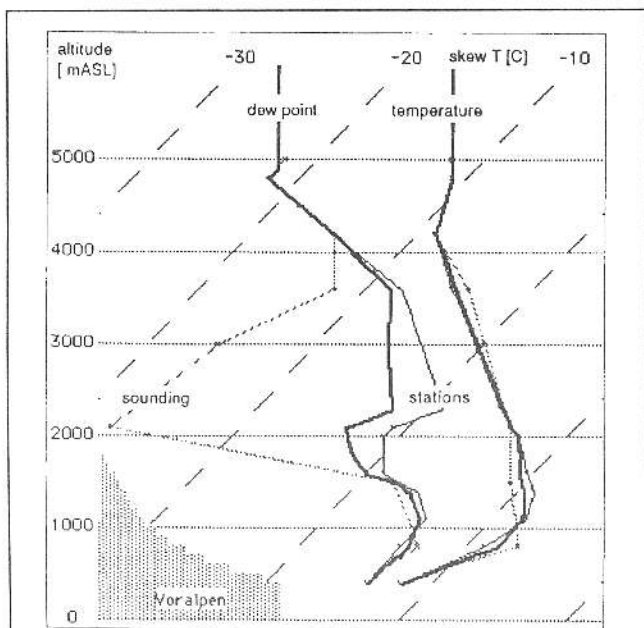


Figure 2. Representative profiles (full, thick lines) as weighted superpositions of radiosonde and ground data. Above topography the higher alpine stations are given higher weight in this case as they all show higher dew points.

point is instructive in cases of dry upper level air as it shows the mixing down of dry air superimposed on the evaporation of water at the ground.

Example 1: Formation of Cumulus Clouds under Subsidence

Subsidence is a crucial parameter for the formation of convective clouds. Starting with identical initial profiles (Figure 3, high pressure building up, dry air above 1500 mASL) <<ALPTHERM>> was run with 4 different values for the subsidence rate: 0, 5, 10, and 20 m/h (Figure 4). Without subsidence, perfect gliding conditions develop with 1 - 2/8 of shallow cumulus clouds. Even a small value of 5 m/h is sufficient to clearly reduce the vertical extension of cumuli and to reduce the cloud

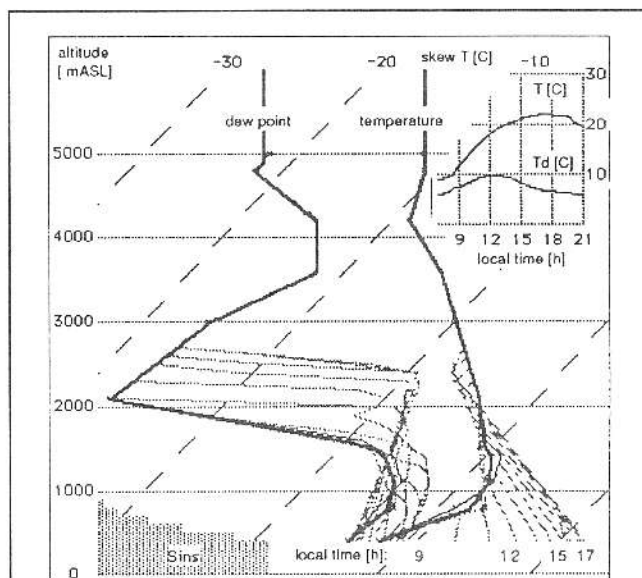


Figure 3. Diurnal evolution of the vertical profiles of temperature and dewpoint over the Swiss plateau on a spring day (left). Time-height cross section (right) of lift rates [0.5 m/s], cumulus clouds, and cloud cover [octas]. Ground values (upper right) of temperature T and dewpoint Td.

cover to 0 - 1/8. At a subsidence rate of 10 m/h clouds form shortly around 1 pm and again after 4 pm. At subsidence rates of 20 m/h and higher, no convective clouds develop. If the subsiding dry air aloft is accompanied by a temperature inversion above the moist air, the top height of dry thermals and the lift rates will also be reduced.

Example 2: Enhancement of an Inversion in a Valley

In air quality issues the breaking of low lying inversions is of great importance. The following example shows that valley inversions are temporarily enhanced by convection if the top of the inversion lies within topography (Figure 5). The presented example shows an area-height distribution at the northern border of the Swiss pre-Alps. It is typical for the lower parts of important alpine valleys. The area-height distribution extends

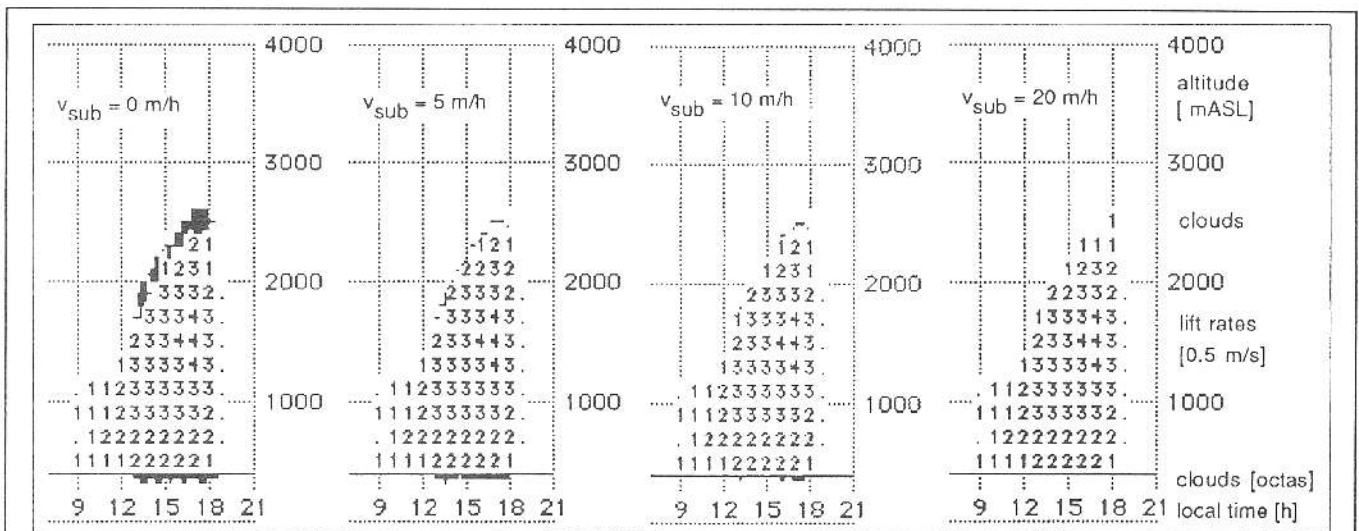


Figure 4. Effects of subsidence on the formation of cumulus clouds. Subsidence rates of 0, 5, 10, and 20 m/h were applied from left to right. Cloud cover [octas] is indicated at the bottom of the time-height cross section.

from 400 mASL to 1800 mASL, the average height being about 900 mASL. At sunrise the top of the inversion is found around 1100 mASL with a maximum temperature of 12 °C. Below 1100 mASL the lapse rate is 0.55°C / 100m, above 2000 mASL it is -0.65°C / 100m. A first observation after sunrise is the formation of two decoupled convective regimes separated by the top of the inversion. A second observation is that the temperature above the inversion increases and that the warmest point in the profile gradually rises to 1300 mASL - the inversion is enhanced by the convection generated above the inversion. Between 1100 and 1900 mASL this enhancement is indicated by the hatched part to the right of the initial temperature profile. Eventually the valley thermals push through the enhanced inversion and form clouds at 2300 mASL after 2 pm. With the low lapse rate found above the condensation level the clouds grow rapidly to more than 4000 mASL, cloud cover 1-3/8. The mixing down of dry air to the valley floor is reflected in the dew point curve after 1:30 pm.

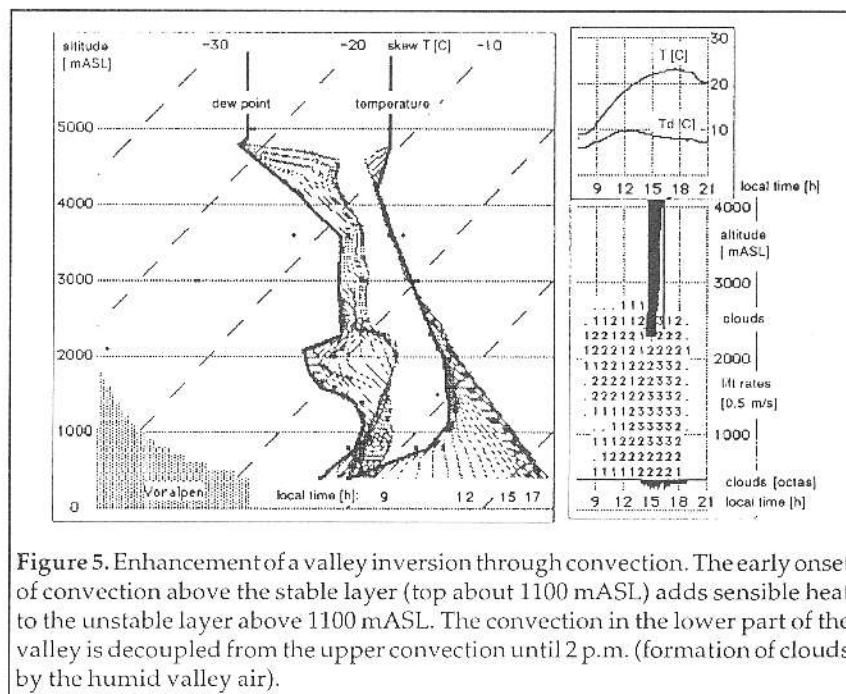


Figure 5. Enhancement of a valley inversion through convection. The early onset of convection above the stable layer (top about 1100 mASL) adds sensible heat to the unstable layer above 1100 mASL. The convection in the lower part of the valley is decoupled from the upper convection until 2 p.m. (formation of clouds by the humid valley air).

Example 3: Volume Effect

In order to demonstrate the volume effect <<ALP THERM>> may be applied to an isothermal profile over different topographies. The apparent increase of sensible heat as deduced from the skew T-altitude diagram is due to the volume effect (Figure 6). The depth of the mixed layer is larger over complex topography. Again the convective warming at higher altitudes temporarily transforms the isothermal stratification into an inversion.

The operational use of <<ALP THERM>> as a forecasting tool for gliding was tested during the Swiss Nationals in May 1993. At the daily briefing forecast

time-height cross sections of thermals (Table 2) were presented by the national weather service for the three contest regions plateau, Jura, and pre-Alps. Contestants were highly interested and participated in the test by handing in barograms and weather reports with information on lift rates, cloud cover and height of cloud base as a function of daytime and region. Analysis of the data is in process. The importance of sub-

time hh:mm	temp [C]	dewp [C]	altitude [km], lift rate [0.5 m/s], Cu [°]				clouds [octas]	base [m]	top [m]
			1	2	3	4			
7.30	9.1	6.1							
8.00	9.5	6.2							
8.30	10.6	6.5							
9.00	11.8	7.0	-11.1:1						
9.30	12.6	7.5	-11.1:1						
10.00	14.0	8.1	-111.1:1						
10.30	15.1	8.7	-11111:1						
11.00	16.1	9.2	-12222:.						
11.30	17.1	9.5	-12222:11						
12.00	17.9	9.6	-12222:221						
12.30	18.6	9.7	-22222:32211						
13.00	19.2	9.6	-22223:333221*1			*	1700	1700	
13.30	19.8	9.5	-22223:333322***			*	1800	2000	
14.00	20.2	9.4	-22223:3333332*			*	1900	1900	
14.30	20.6	9.0	-22223:33333333***			*	2000	2200	
15.00	21.0	8.5	-22223:333333333**			*	2100	2200	
15.30	21.3	8.0	-22223:333343333*21*			*	2300	2300	
16.00	21.5	7.6	-22223:333444433:32**			*	2300	2400	
16.30	21.7	7.3	-22223:334444433:32***			*	2300	2500	
17.00	21.9	7.1	-22223:334444443:33***			*	2300	2500	
17.30	22.0	7.0	-22223:334444443:332***			*	2400	2600	
18.00	21.8	6.9	-1222:333333333:222**			*	2400	2500	
18.30	21.6	6.8	..111:11111111:11						
19.00	21.5	6.6							
19.30	21.5	6.6							
20.00	20.8	6.4							
20.30	20.0	6.3							
21.00	19.6	6.3							

Table 2. <<ALPTHERM>> gliding forecast.

sidence on the formation of clouds was clearly recognized (Example 1). For the contest director the model provided important information about take-off time and the end of convection in the different contest regions. Under unstable conditions the towering up of the

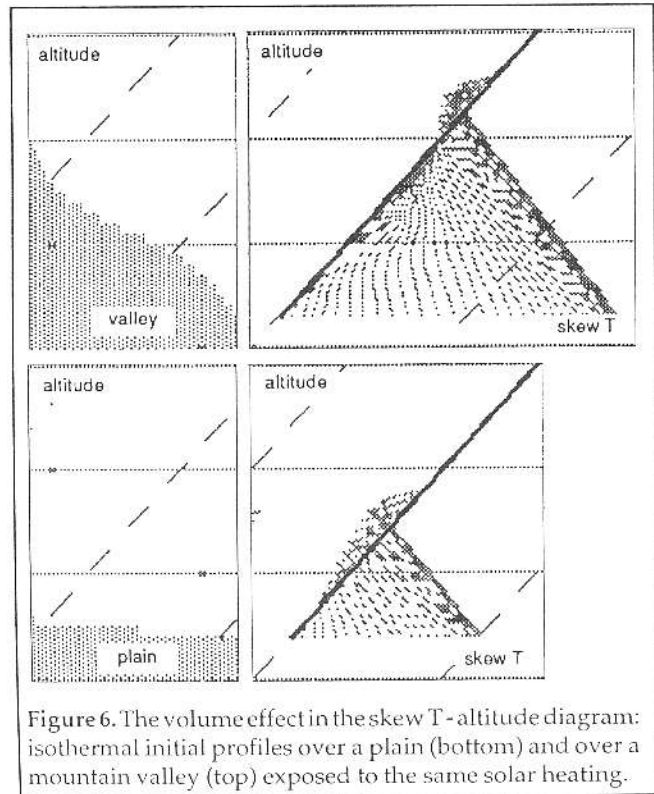


Figure 6. The volume effect in the skew T-altitude diagram: isothermal initial profiles over a plain (bottom) and over a mountain valley (top) exposed to the same solar heating.

convective clouds could be estimated for the different regions and the tasks set accordingly.

Conclusions

Topography is a key element for regionalized gliding forecasts. Its detailed consideration in modelling atmospheric convection is possible with today's personal computers. The presented PC-based model <<ALPTHERM>> produces regionalized forecasts of the parameters important for gliding. Used as a simulator <<ALPTHERM>> illustrates effects like the convective enhancement of low-lying inversions in mountain valleys and the volume effect. Quantitative information of the mixing process in the

boundary layer is also obtained for complex topography.

References

Truog, G. (1979): Handbuch für die Segelflugprognose. Arbeitsbericht No. 88 der Schweizerischen Meteorologischen Anstalt.

Neininger, B. (1982): Mesoklimatische Messungen im Oberwallis. Annalen der Meteorologie 19.

Whiteman, C.D. (1982): Breakup of temperature inversions in deep mountain valleys. Journal of Applied Meteorology, 21, 270-289.

Neininger, B. and Liechti, O. (1983): Mesoscale Measurements for gliding forecast in an alpine valley. OSTIV Publication XVII.

Steinacker, R. (1984): Area-height distribution of a valley and its relation to the valley wind. Beitr. Phys. Atmosph., 57, 64-71.

Liljequist, G.H. and Cehak, K.: Allgemeine Meteorologie. Vieweg Verlag (1984), ISBN 3-528-23555-1.

Hackel, H.: Meteorologie. Uni-Taschenbucher für Wissenschaft 1338, Verlag Eugen Ulmer (1990), ISBN 3-8001-2610-9.

OSTIV (1993): Handbook of Meteorological Forecasting for Soaring Flight, Revision of WMO Technical Note 158.